IEEE Open Journal of
Ultrasonics, Ferroelectrics, and Frequency Control

Received 12 September 2022; revised 17 November 2022 and 31 January 2023; accepted 16 March 2023.
Date of publication 20 March 2023; date of current version 31 March 2023.

Digital Object Identifier 10.1109/OJUFFC.2023.3259941

Quantification of Flow Rates and Flow Volumes in Valve Regurgitation Using 3-D High Frame-Rate Ultrasound

STEFANO FIORENTINI[1,2], ERIK ANDREAS RYE BERG[1,2,3], HANS TORP[1,2] (Member, IEEE), SVEND AAKHUS[1,2,3], AND JØRGEN AVDAL[1,2,4] (Member, IEEE)

[1]Department of Circulation and Medical Imaging, Norwegian University of Science and Technology (NTNU), 7030 Trondheim, Norway
[2]Centre for Innovative Ultrasound Solutions (CIUS), 7030 Trondheim, Norway
[3]Clinic of Cardiology, St. Olavs Hospital, 7030 Trondheim, Norway
[4]Department of Health Research, SINTEF Digital, 7465 Trondheim, Norway
CORRESPONDING AUTHOR: S. FIORENTINI (stefano.fiorentini@ntnu.no)

This work involved human subjects or animals in its research. Approval of all ethical and experimental procedures and protocols was granted by the Regional Committee for Medical and Health Research Ethics (REK) under Protocol No. 2017/900.

ABSTRACT Valve regurgitation is a cardiac condition caused by the incomplete closure of a cardiac valve. Untreated, this condition may result in cardiac failure. Regular monitoring of this condition is essential in guiding the decision process for surgical intervention. Current guidelines recommend a multi-parametric assessment of valve regurgitation using echocardiography, which is both time consuming and heavily dependent on the experience of the examiner. Several methods have been proposed to provide quantitative markers to facilitate the assessment of valve regurgitation, most notably the Proximal Isovelocity Surface Area (PISA) method and methods based on the quantification of the total Regurgitant Volume (RVol) from the power of backscattered blood signal. In this work, we propose a framework based on trans-thoracic 3-D high frame-rate acquisitions for the simultaneous estimation of the jet cross-sectional area and jet velocity directly at the jet core, which are then combined to estimate the instantaneous flow rate and RVol patients with aortic or mitral insufficiency. We compare two methods for the segmentation of the jet cross-sectional area from the power Doppler signal. Validation on simulated data indicates good segmentation accuracy for the best method ($\boldsymbol{\beta} = 0.97$, $\boldsymbol{R}^2 = 0.91$). Validation on recordings from a flow phantom shows good agreement ($\boldsymbol{\beta} = 1.2$, $\boldsymbol{R}^2 = 0.88$) with an external flow rate meter. Clinical feasibility of the method is also shown in a patient with mitral regurgitation.

INDEX TERMS Blood velocity estimation, flow rate quantification, segmentation, ultrasound doppler, valve insufficiency.

I. INTRODUCTION

VALVE regurgitation is a cardiac condition caused by the incomplete closure of a cardiac valve. Untreated, this condition leads to a cascade of events that may result in cardiac failure. Regular monitoring of this condition is essential in the decision process for surgical intervention [1], [2].

Current recommendations suggest an integrative, multi-parametric assessment of valve regurgitation using echocardiography [3], [4]. The procedure currently involves the evaluation of valve morphology and a variety of quantitative and semi-quantitative indices based on Color Flow, Pulsed Wave (PW) Doppler and Continuous Wave (CW) Doppler. As a result, valve regurgitation assessment is heavily dependent on the examiner's experience and can be a cumbersome procedure. The multitude of recommended markers could be regarded as a sign of the complexity of valve disorders. Arguably, it is also a consequence of the lack of a reliable quantitative method.

Among the available quantitative markers for valve regurgitation assessment, the total Regurgitant Volume (RVol) and EROA are the most commonly used. An established method

for the assessment of RVol and EROA is the Proximal Isovelocity Surface Area (PISA) method [3], [5], [6], [7], [8], [5], [9], [10], [11], [12], [13], [14], [15], [16]. When using the PISA method, the orifice is assumed to be circular and planar, mass is conserved, and both source and sink chambers are sufficiently large. With these assumptions fulfilled, it can be shown that flow accelerates towards the orifice forming isovelocity hemispheres. The instantaneous flow rate can then be estimated from 2-D Color Flow by measuring the diameter of the aliased velocity region. The Effective Regurgitant Orifice Area (EROA) is estimated by dividing the instantaneous flow rate by the peak velocity estimated from CW Doppler. Finally, the Regurgitant Volume (RVol) is calculated as the velocity time integral over the regurgitation phase multiplied with the estimated EROA.

Several limitations of the PISA method are documented in the literature [3], [5], [17], [18], [19], [20], [21], [22], [23], [24], [25], [26], [27], [28], [29], [30], including incorrect assumptions about the orifice morphology, dependence on user-defined parameters such as Pulse Repetition Frequency (PRF) and gain, and angle dependency of Color Flow estimates. Moreover, due to workload constraints, the EROA is often estimated from a single frame and assumed constant during the entire regurgitation phase, which is often not correct [3], [4]. Nevertheless, studies have shown both modest inter-observer agreement [31] and modest intra-observer agreement on repeated assessment of single-view loops [32]. 3-D Color Flow was proposed to improve PISA and RVol estimates in non-circular orifices [33], [34], but these techniques are not yet widely used clinically.

More recently, a number of methods combining transesophageal 3-D Color Flow and more refined assumptions on the flow field have been proposed. In the 3-D Field Optimization Method (3-D FOM) [35] the flow field in the convergence region, still assumed as hemispheric, is estimated by performing an automated frame-by-frame fit between modelled and observed Color Flow velocities. 3-D FOM achieved good agreement with an external flow meter in an experimental setup [36] and with 2-D PISA in a clinical study [37]. In a later development by Militaru et al. [38] assumptions on the shape of the flow convergence regions were removed by using a flow model based on a simplified version of the Navier-Stokes equations. In recent work by Singh et al. [39] the flow model was further refined by providing a 3-D segmentation of the valve geometry from B-Mode as boundary conditions. Although promising, these methods currently rely on transesophageal recordings, which limits their daily use in the clinics.

Other research studies attempted the direct quantification of EROA and Rvol at the jet core [40], [41], [42]. Assuming laminar flow and constant hematocrit, the volume of blood within a sample volume of an ultrasound beam is proportional to the back-scattered power from red blood cells after clutter filtering. After performing a calibration procedure, the backscattered blood signal at the jet core can be used to estimate the jet Cross Sectional Area (CSA). Once the jet CSA is known, the instantaneous flow rate and RVol can be calculated by multiplying the jet CSA by the Velocity Time Integral (VTI) from CW Doppler. This method was investigated *in vivo* using single beam, focused, high PRF (HPRF) acquisitions [43], [44], [45].

One known limitation of this method is the inability to evaluate jets larger than the beam CSA. Although reducing the active aperture can be used to expand the ultrasound beam at the cost of signal strength, the application of the method remains precluded to severe insufficiencies, as well as non-severe insufficiencies with slit-like orifice. After discarding orifice sizes exceeding the beam width, studies have shown good agreement with MRI [18], [44]. Multi-beam, focused, 3-D high PRF acquisitions have been investigated using matrix array transducers, to overcome the limitations of single-beam acquisitions, also showing good agreement with MRI [46], [47], [48].

In this work, we propose a trans-thoracic acquisition setup and a processing chain to estimate the jet CSA, the instantaneous flow rate and the total Regurgitant Volume (RVol) directly at the jet core, in patients with aortic or mitral insufficiency. As first suggested by Avdal et al. [49], we propose to estimate the flow rate by first segmenting the cross-sectional power Doppler image of the jet. By using unfocused beams, 3-D Doppler data can be acquired continuously rather than using packets, enabling the simultaneous estimation of blood velocities and jet cross-sectional area. Two methods for the segmentation of the jet CSA are proposed. Moreover, two transmit beam configurations and their impact on segmentation performance are investigated. The pipeline is validated using simulated data and experimental recordings from a jet phantom. Finally, clinical feasibility is shown in a patient with mitral regurgitation.

The acquisition setup and methods are described in section II. The validation on experimental and simulated data, and the clinical feasibility study are described in Section III. The results are presented in Section IV and discussed in Section V.

II. METHODS

In the proposed method, the instantaneous flow rate Q is estimated from continuous, unfocused 3-D ultrasound recordings, by numerically estimating the following integral over a cross sectional slice of the jet parallel to the transducer surface.

$$Q = \int_{\Sigma} v(x, y)\, dxdy \tag{1}$$

where $v(x, y)$ is the axial velocity estimate at coordinates (x, y). The velocity is estimated from the PW Doppler spectrum at coordinates (x, y) using the procedure explained in Section II-B. Σ denotes the integration support, which is segmented from the power Doppler signal of the jet, as explained in Section II-D. A schematic representation of

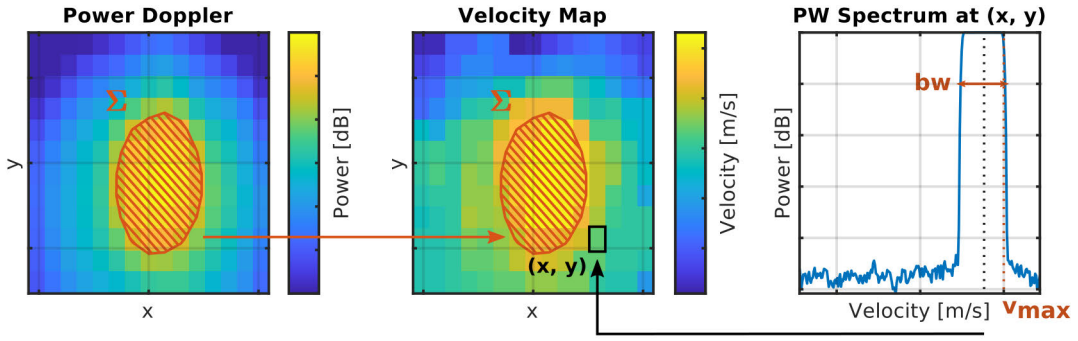

FIGURE 1. **Schematic representation of the flow rate estimation procedure. The instantaneous flow rate is estimated as the integral of the estimated velocity map shown in Panel B enclosed in the segmented jet area (orange slashed region show in panel A). Panel C shows the PW Doppler spectrum estimated at the pixel highlighted in black in panel B. The black dashed line shows the velocity estimate used for the flow rate calculation, along with the estimated maximum velocity (orange vertical line) and bandwidth (orange horizontal line).**

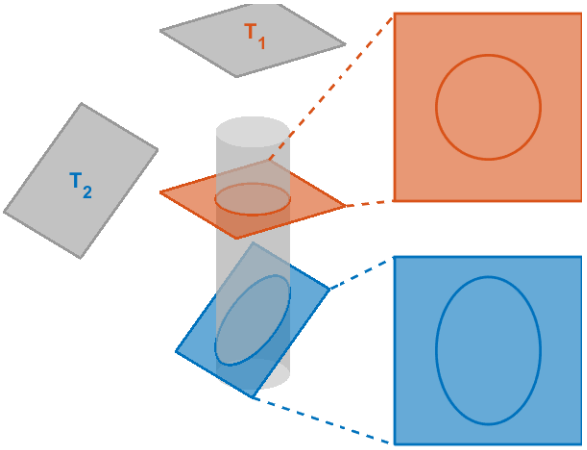

FIGURE 2. **Schematic depiction of a jet (gray cylinder) imaged by two transducers, with surfaces T_1 and T_2. As the beam-to-flow angle θ increases (blue plane), the cross sectional area of the sliced cylinder increases by a factor $1/\cos\theta$. On the other hand, the estimated phase shift from PW Doppler decreases by a factor $\cos\theta$. The instantaneous flow rate, being the product of the two, is therefore angle independent.**

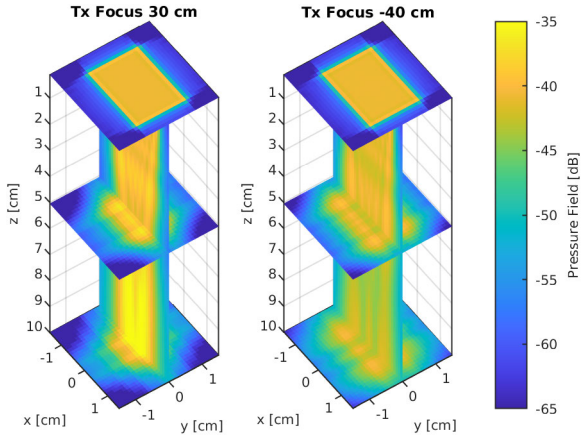

FIGURE 3. **Simulated 3-D pressure fields, using the GE 4Vc-D transducer geometry and the acquisition parameters given in Table 1. Left panel: tx focus set 30 cm in front of the transducer. Right panel: focus set 40 cm behind the transducer.**

the flow rate estimation in Eq. (1) is shown in Fig. 1. Finally, the total regurgitant volume (RVol) is obtained by numerical integration of the instantaneous flow rate Q over the regurgitation period T

$$RVol = \int_T Q(t)\,dt \tag{2}$$

whereas the jet CSA is estimated as the area of Σ

$$CSA = \int_\Sigma dxdy \tag{3}$$

As illustrated for the case of a cylindrical jet in Fig. 2, as the insonification angle θ varies, the velocity estimated from PW Doppler varies by a factor $\cos\theta$, whereas the observed cross-sectional area varies by $1/\cos\theta$. Therefore, the flow rate estimated using Eq. (1) is not dependent on the insonification angle.

A. ACQUISITION SETUP

Ultrasound data were recorded using a GE E95 scanner (GE Vingmed AS, Horten), equipped with a GE 4Vc-D matrix transducer (0.16 mm azimuth pitch, 0.23 mm elevation pitch, 100 azimuth elements, 60 elevation elements, 2.8 MHz center frequency). The software was locally modified to enable high frame-rate acquisitions. Two transmit configurations were evaluated for this application, one using weakly focused beams, and one using diverging beams. The focal points for the transmitted beams were 30 cm in front of the transducer and 40 cm behind it, along the central axis. Beam profiles for the two configurations are shown in Fig. 3. Moreover, high-PRF mode was enabled to prevent aliasing, at the cost of spatial ambiguity. A summary of the acquisition parameters is given in Table 1. For every recording, 1 second of IQ channel data were stored for off-line processing. Chan-

TABLE 1. Acquisition parameters.

Parameter	Symbol	Value
Transmit frequency	f0	2 MHz
Number of pulse cycles at f0	Nc	3.5
Pulse repetition frequency	PRF	[12, 18] kHz
Demodulation frequency	fd	2.9 MHz
Sampling frequency	fs	4.5 MHz

nel data were beamformed using the UltraSound ToolBox (USTB). To avoid erroneous calculations of the jet area under the presence of recruited flow, beamformed data were clutter filtered to preserve velocities above 70% of the maximum velocity in the PW Doppler spectrum. PW Doppler spectra and power Doppler were generated using the same temporal observation window for every voxel at a manually defined depth. Cross-sectional jet area and flow rates were estimated using the approaches described in Section II. A summary of the post-processing parameters is given in Table 2.

B. BLOOD VELOCITY ESTIMATION

In this framework we used the mean velocity to quantify the flow rate. Rather than using a lag-1 autocorrelation estimator, we estimated the mean velocity from the PW Doppler spectrum as

$$\hat{v} = v_{max} - \frac{bw}{2} \tag{4}$$

where v_{max} is the maximum velocity envelope in the spectrum, estimated as the highest velocity value with intensity above an user-defined threshold above the noise floor, based upon visual inspection of the maximum velocity envelope trace, and bw is the bandwidth of the PW Doppler spectrum, estimated as the number of velocity samples above the same power threshold used for the identification of v_{max}. A depiction of the estimated maximum velocity and bandwidth in a PW spectrum is given in Fig. 1, panel C.

C. DEPTH ESTIMATION

Because of potential movement of the valve throughout the regurgitation phase, it is necessary to follow the movement of the jet core. This is achieved in a two-step approach. First, the maximum velocity envelope from the PW Doppler spectrum is traced in every voxel. Second, the position of the jet core is estimated as the centroid of the volume that contains the 75% highest velocities. Finally, the jet cross-section is segmented according to Section II-D along a plane perpendicular to the transmit beam direction and passing by the estimated centroid depth.

D. CROSS-SECTIONAL AREA ESTIMATION

We investigated two methods for segmenting the cross-sectional area of a jet from its power Doppler signal.

1) −3 dB THRESHOLD

In the 1-D case, assuming the spatial invariance of the Point Spread Function (PSF) and a large object size compared to the PSF, the −3 dB power level coincides with the contour of the object. A visual depiction is given in Fig. 4. Under the aforementioned assumptions, the area enclosed within the −3 dB contour will provide an estimate of the jet cross sectional area.

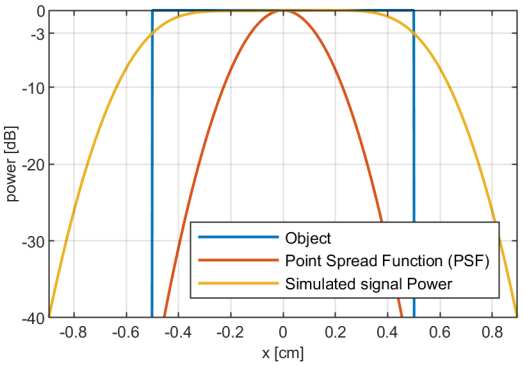

FIGURE 4. 1-D example showing the power Doppler depiction (yellow) obtained from the convolution of the object function (blue) with the PSF (orange). It can be noticed that, provided that the object is larger than the PSF, the −3dB coincides with the contour of the object.

2) ITERATIVE RECONSTRUCTION METHOD

The shape and position of the object is estimated using an iterative approach that maximizes the 2-D normalized cross-correlation (NCC) between the observed power Doppler image and a synthetic power Doppler that the estimated object would generate given the current imaging conditions

$$\text{NCC} = \frac{1}{N}\sum_{x,y}\frac{(f(x,y)-\mu_f)(g(x,y)-\mu_g)}{\sigma_f\sigma_g} \tag{5}$$

where N is the total number of pixels in each of the two images, f and g are the observed and synthetic power Doppler images respectively, and μ and σ denote mean and standard deviation of the two images. The maximum for the normalized cross correlation is found using the direct search method described in [50], which does not require numerical evaluation of the gradient of the cost function.

A simulation approach based on averaging the power of the backscattered signal from randomly distributed scatterers would take a considerable amount of time to be feasible for practical purposes. The proposed method instead generates a power Doppler depiction of a given object by numerical integration of the power of the pulse-echo response for each pixel

$$g(x,y) = \iint_{\Sigma} P_h(x,y,w,v)\,dw\,dv \tag{6}$$

where g denotes the power Doppler image of the object, x and y are the power Doppler image coordinates, Σ denotes the object surface, and P_h is the power of the pulse-echo

response, calculated as

$$P_h(x, y, w, v) = \int_{-\infty}^{+\infty} |\mathrm{h}(x, y, w, v, t)|^2 \, dt \tag{7}$$

where h() denotes the pulse-echo response, calculated using Field II. Numerical integration is performed along fast time t. The pulse-echo response is evaluated at coordinates (w, v), which should define a finer grid than (x, y) for accurate results. It should be noted that, assuming dynamic receive focusing, the pulse-echo response must be calculated for every (x, y) in the power Doppler image. The power of the pulse-echo response is computed before the iterative reconstruction method takes place and is specific to the combination of transducer geometry, impulse response, imaging depth and acquisition setup. Throughout this work we used the acquisition parameters presented in Section II-A to generate the pulse-echo response used in the method. Provided that the imaging parameters do not change during acquisition, the same pulse-echo response power can be reused. Furthermore, only elliptical objects are modelled. This choice reduces the number of parameters explored by the optimization algorithm to five: major axis a, minor axis b, orientation θ and center coordinates (x_0, y_0). A schematic representation of the method is given in Fig. 5.

III. VALIDATION

A. SIMULATIONS

A validation based on simulated data was performed with two purposes in mind. First, to verify that the fast power Doppler simulator could replicate results from a conventional simulation approach such as Field II. Second, to benchmark the iterative reconstruction approach against thresholding. The methods described in Section II-D to segment the jet and estimate the cross-sectional area were tested on a set of 100 images, each representing the cross-sectional power Doppler of a jet. The source objects were modelled as ellipses, with geometric properties representative of valve insufficiencies with different severity. RF channel data of each object were simulated in Field II [51], using the GE 4Vc-D transducer geometry and the acquisition parameters given in Table 1. The objects were populated with point scatterers according to a uniform random distribution to achieve and approximate density of 10 scatterers within the -6dB contour of the Point Spread Function. This condition was chosen to ensure Gaussian distributed channel data. Channel data were beamformed using the UltraSound ToolBox (USTB). Finally, the power Doppler image of each object was generated by averaging 100 independent realizations to simulate a long observation window and achieve low variance in the final power Doppler image.

B. PHANTOM EXPERIMENT

The experimental setup used to validate the flow rate estimation algorithm is shown in Fig. 6. The setup consisted of two fluid reservoirs, one acting as source and the other

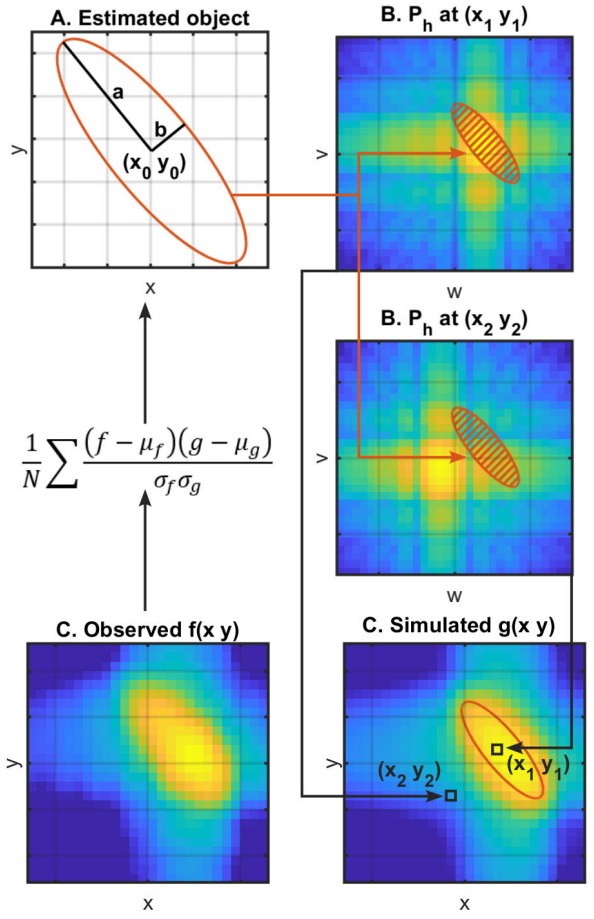

FIGURE 5. Schematic representation of the iterative reconstruction method. At the start of a new iteration, a guess for the underlying jet cross-section is made (Panel A), and a power Doppler depiction of that (Panel C) is generated by numerical integration of the pulse-echo power P_h, which is computed beforehand for every pixel (x, y) in the imaging grid using Field II (Panel B). Finally, the normalized cross-correlation between the observed power Doppler $f(x, y)$ and the simulated power Doppler $g(x, y)$ is calculated. A direct search optimization algorithm adjusts the geometric parameters of the jet cross-section to maximize the normalized cross correlation.

TABLE 2. PW doppler processing parameters.

Parameter	Symbol	Value
Observation window length	Δt	10 ms
Window function		Kaiser
Overlap		50%
Clutter Filter		FIR
Filter order		220
Temporal Smoothing	Ns	11 samples

as drain, a replaceable orifice model enclosed in a box with an acoustic window, and a peristaltic pump (model 10-10-00, Stockert-Shiley). A transit-time, ultrasonic flow meter (model UF25B, Cynergy3) was installed before the orifice phantom to provide reference flow rate measurements. The flow setup was filled with a mixture of corn starch and

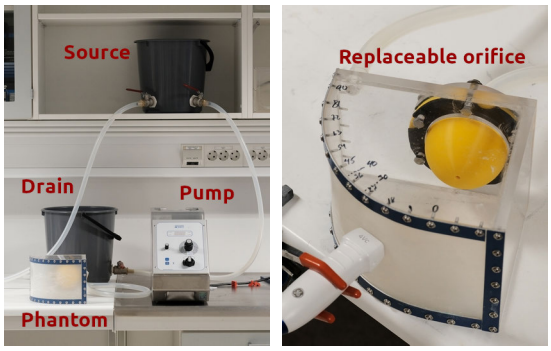

FIGURE 6. Left panel: overview of the experimental setup. Right panel: close up view of jet phantom. The orifice model can be replaced to accommodate different sizes and shapes. A large, curved, acoustic window allows the user to record the jet from a wide range of beam-to-flow angles.

water with a ratio of 5 g/L to replicate the scattering properties of blood. The height difference between source and drain reservoirs determined the pressure drop across the phantom and could be adjusted to achieve different flow rates. Three height differences were tested, 65 cm, 100 cm, and 135 cm. The phantom allowed the user to replace the orifice model to validate the method against different orifice sizes. In this work we performed recordings from circular orifices with 0.15 cm^2, 0.25 cm^2, 0.35 cm^2 and 0.45 cm^2 cross-sectional area, representing valve insufficiencies of different severity. The wide acoustic window allowed the user to record data at different insonification angles. We performed recordings at 0°, 30°, 40° and 50° beam-to-flow angle, which should cover even the more challenging cases in clinical practice. For each combination of angle and orifice size, three different flow rates values were achieved by placing the source reservoir at predefined heights. The imposed pressure difference remained the same for the different orifice models. Consequently, each orifice model resulted in different ranges of achieved flow rates, with the smaller orifice achieving lower flow rates due to higher flow resistance.

C. CLINICAL FEASIBILITY ANALYSIS

Feasibility of the estimation method and the acquisition setup described in Section II were tested in a patient with mitral regurgitation. The study was approved by the Regional Committee for Medical and Health Research Ethics (REK) with protocol number 2017/900, and the patient provided informed written consent before the recording took place. Channel data were recorded by an expert echocardiographer using a GE E95 scanner equipped with a GE 4Vc-D matrix transducer (GE Vingmed AS, Horten). The scanner was locally modified to enable high frame-rate acquisitions. The transmit focus was placed 40 cm behind the transducer to achieve diverging beams, and high-PRF mode was enabled to prevent aliasing. The Pulse Repetition Frequency (PRF) was approximately 12 kHz. Around 2 seconds of channel data were stored for offline processing. The instantaneous flow rate was estimated

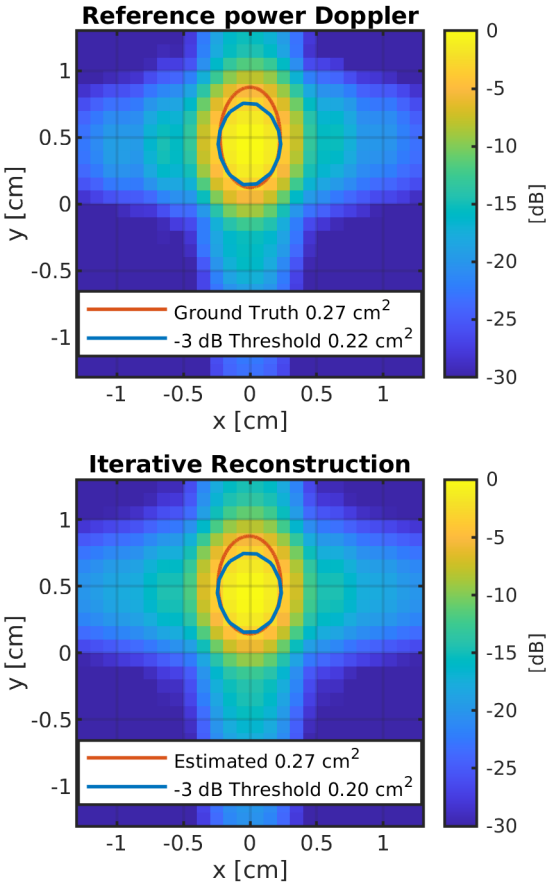

FIGURE 7. Comparison between a reference power Doppler Image, simulated by averaging the signal power from 100 independent realizations simulated using Field II (upper panel), and the power Doppler image generated by the iterative reconstruction method (lower panel). Visual comparison between the simulation methods highlights minor differences in the sidelobes but not in the main lobe. The true and estimated object contours are presented, as well as the −3dB contour.

using the approaches explained in Section II, and the total regurgitant volume (RVol) was estimated by numerical integration of the flow rate curves. An expert echocardiographer estimated EROA and flow rate from the same patient using the 2-D PISA method. The total regurgitant volume (RVol) was estimated by multiplying the estimated EROA from 2-D PISA by the velocity time integral (VTI) from CW Doppler. The clinical analysis was performed using ECHOPAC (version 204, GE Vingmed AS, Horten).

IV. RESULTS

A. IN SILICO VALIDATION

In Fig. 7 the power Doppler image simulated using Field II is compared against the power Doppler image simulated using the iterative algorithm presented in Section II-D. The estimated normalized cross correlation in the example was 0.99. The reference and estimated objects are shown, as well as the −3 dB segmentation result from the power

Doppler image. It can be noticed that the −3 dB segmentation suggests a smaller cross-sectional area than the iterative method, which matches the reference object more closely. It can be also noticed that the power Doppler image simulated by integration of the pulse-echo response (lower panel) appears similar to the reference (upper panel), which was instead simulated using Field II by averaging independent realizations from randomly distributed scatterers. Visual comparison between the simulation methods highlights minor differences in the sidelobes but not in the main lobe.

In Fig. 8 the area estimates using a −3 dB threshold and the iterative reconstruction method are compared on a set of 100 objects mimicking the cross-section of insufficiency jets of varying severity. Results indicate that using a slightly diverging beam on transmit yields better correlation and reduced bias, compared to a weakly focused transmit beam. Similarly, the iterative reconstruction method yields better overall fit ($y_0 = 0.00, \beta = 0.97, R^2 = 0.91$) compared to a −3 dB threshold ($y_0 = 0.08, \beta = 0.58, R^2 = 0.71$). Moreover, the presence of a non zero intercept y_0 in the −3dB threshold approach suggests that this method may inherently overestimate small orifices.

B. PHANTOM EXPERIMENT

Fig. 9 shows estimated flow rates using the flow phantom setup and weakly focused waves, versus reference values from a transit-time flow meter. The width of the error bars displays the standard deviation over 50 repeated measurements. Results indicate that the overall fit using this setup is relatively low, but the iterative reconstruction method achieves better correlation ($R^2 = 0.51$) compared to a −3 dB threshold ($R^2 = 0.34$). On the other hand, the increased width of the error bars indicates that the iterative method hardly converges to a stable estimate. Moreover, the regression line for the iterative reconstruction method is closer to the identity line both in terms of slope ($\beta = 0.76$ vs $\beta = 0.69$, respectively) and intercept ($y_0 = 36.92$ vs $y_0 = 44.43$, respectively), although differences are minor.

Corresponding results using diverging beams are shown in Fig. 10. The correlation between estimated and reference flow rates is higher than when using weakly focused beams. The results also indicate that the iterative reconstruction method yields better correlation ($R^2 = 0.88$) compared to a −3 dB threshold ($R^2 = 0.64$). Moreover, results indicate a substantially improved agreement between the regression line and the identity line, both in terms of slope ($\beta = 1.13$ vs $\beta = 0.76$, respectively) and intercept ($y_0 = 5.78$ vs $y_0 = 34.59$, respectively).

C. CLINICAL FEASIBILITY

Fig. 11 shows the results processed from a high frame-rate recording of a patient with mitral regurgitation. The segmented jet cross-sectional area using a −3dB threshold and the iterative reconstruction method are shown at three instants. The flow rate curves estimated using the approaches

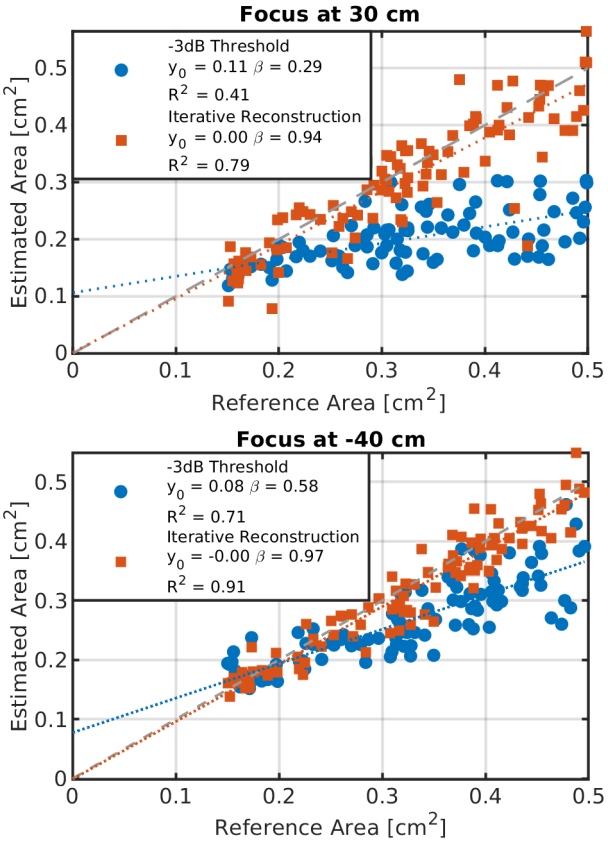

FIGURE 8. Area estimates from the segmentation of power Doppler images using iterative reconstruction (orange squares) and a −3 dB threshold (blue dots) on a set of 100 static targets. The power Doppler image of the targets was obtained by averaging the power independent realizations simulated using Field II and the acquisition parameters given in Table 1.

explained in Section II are also shown. The estimated RVol was 45 ml using a −3 dB threshold and 48 ml using the iterative method. We also estimated the equivalent EROA value by dividing the estimated instantaneous flow rate by the maximum velocity envelope from the PW Doppler spectrum (shown using an orange line in Fig. 11). The equivalent EROA varied between 0.20 cm^2 and 0.38 cm^2 in the regurgitant phase, with an average value of 0.26 cm^2. Fig. 12 presents the results from a 2-D PISA analysis along with a standard 2-D Color Flow image of the mitral valve and a CW Doppler spectrum from the same patient. The estimated RVol from 2-D PISA, averaged over several measurements, was 40 ml, whereas the estimated EROA was 0.2 cm^2.

V. DISCUSSION

In this work we have presented a method for the quantification of jet cross-sectional area, instantaneous flow rate and total regurgitation volume in aortic and mitral regurgitation. The method combines trans thoracic 3-D high frame-rate acquisitions and unfocused beams to perform jet area segmentation and velocity estimation at the jet core from a single recording. The proposed method does not require

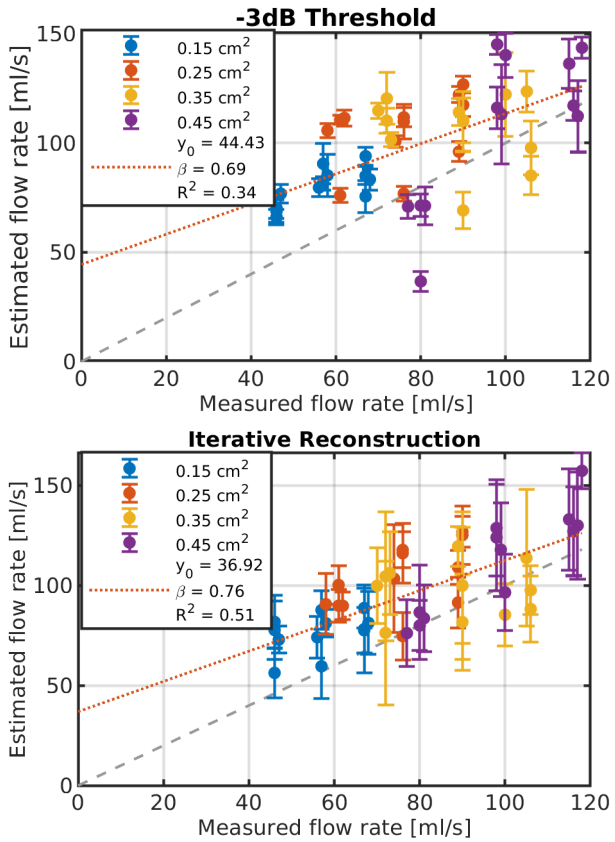

FIGURE 9. Flow rate estimates from the experimental setup described in Section III. The transmit focus was placed 30 cm in front of the transducer. The estimated flow rate from ultrasound is plotted against reference measurements from a reference transit-time flow meter. Each combination of flow rate and beam-to-flow angle is plotted using mean and standard deviation, calculated over 50 repeated measurements. The identity line is shown in grey.

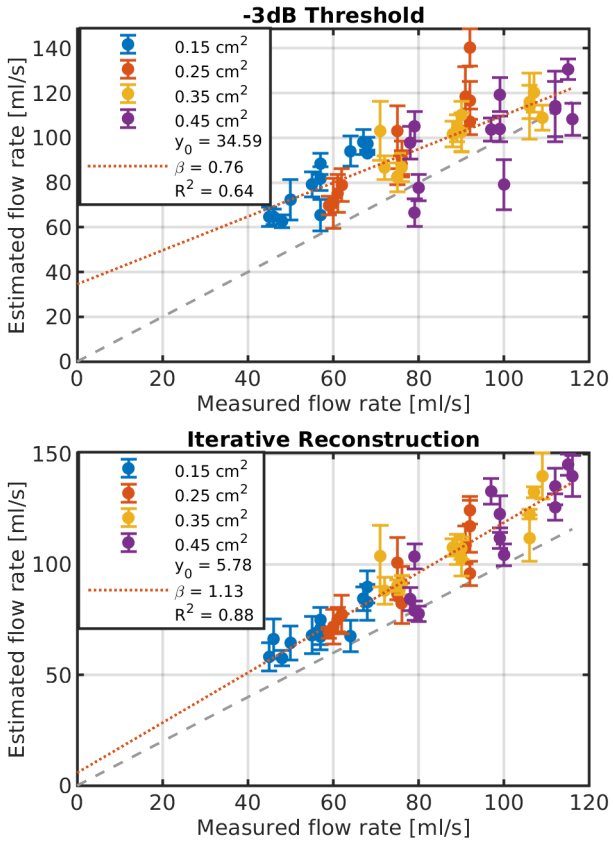

FIGURE 10. Flow rate estimates from the experimental setup described in Section III. The transmit focus was placed 40 cm behind the transducer. The estimated flow rate from ultrasound is plotted against reference measurements from an external transit-time ultrasonic flow meter. Each combination of flow rate and beam-to-flow angle is plotted using mean and standard deviation, calculated over 50 independent measurements. The identity line is shown in grey.

a preliminary calibration procedure as in [18], [43], [44], and [45] and does not require Color Flow recordings at the inflow region as in the PISA method. Moreover, flow rate estimation is performed autonomously at multiple frames throughout the regurgitation phase.

A. ACQUISITION SETUP

Results from both *in silico* validation in Fig. 8 and phantom experiments in Fig. 9 and Fig. 10 indicate that using weakly diverging waves yields better correlation between estimated and reference flow rates than using weakly focused waves. Notably, the area of large orifices are systematically underestimated when using weakly focused beams and a −3dB threshold in Fig. 8. These results can be explained by the improved field uniformity achieved by diverging beams, as shown in Fig 3. Increased transmit beam uniformity ensures a more uniform PSF, which directly benefits the accuracy of both jet segmentation methods.

The results so far suggest that diverging beams should be used in a clinical setup. On the other hand, given the same excitation voltage, diverging beams achieve lower intensity, as shown in Fig. 3. The lower beam intensity results in weaker backscattered signal and limited penetration, which could limit the applicability of the method in patients with challenging imaging conditions. These considerations suggest that the trade off between beam uniformity and penetration depth should be carefully investigated with the aid of simulation programs and water tank measurement.

Finally, enabling high-PRF was necessary to prevent aliasing of the highest jet velocities. It should be noted that depth ambiguity, a side effect of this acquisition modality, does not constitute a problem in this application, because the high velocities of interest ($v > 1$ m/s) can only be related to insufficiency jets.

B. DEPTH ESTIMATION

As reported in Section II-C, the flow rate is estimated at the depth of the centroid of the volume containing the 75% highest velocities from PW Doppler. Due to possible asymmetric velocity distributions at the convergence region, this approach

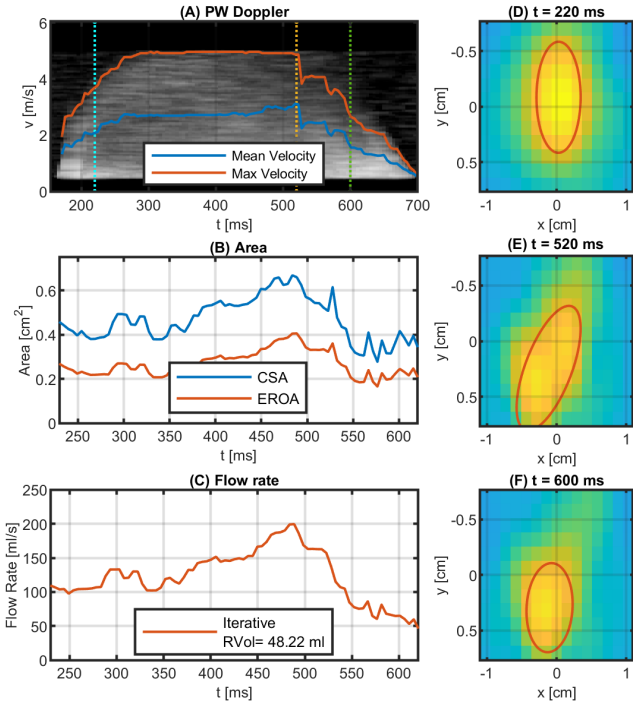

FIGURE 11. Example from a patient with mitral regurgitation. Panels D, E and F show three cross-sectional power Doppler depictions of the regurgitant jet along with the segmentation results from the iterative method (orange ellipses). The three images are processed at the instants indicated by the vertical lines in the PW Doppler spectrum (Panel A). Panel C shows the flow rate curve estimated from the combination of the jet CSA estimate from iterative method (blue line in Panel B) and the mean velocity estimate from PW Doppler (blue line in Panel A). RVol was obtained by numerical integration of the flow rate curve was 48 ml. Finally, Panel B displays the jet CSA against the equivalent EROA (orange line), estimated by dividing the instantaneous flow rate by the maximum velocity envelope from the PW Doppler spectrum (orange line in Panel A). The average equivalent EROA over the regurgitation phase was 0.26 cm^2.

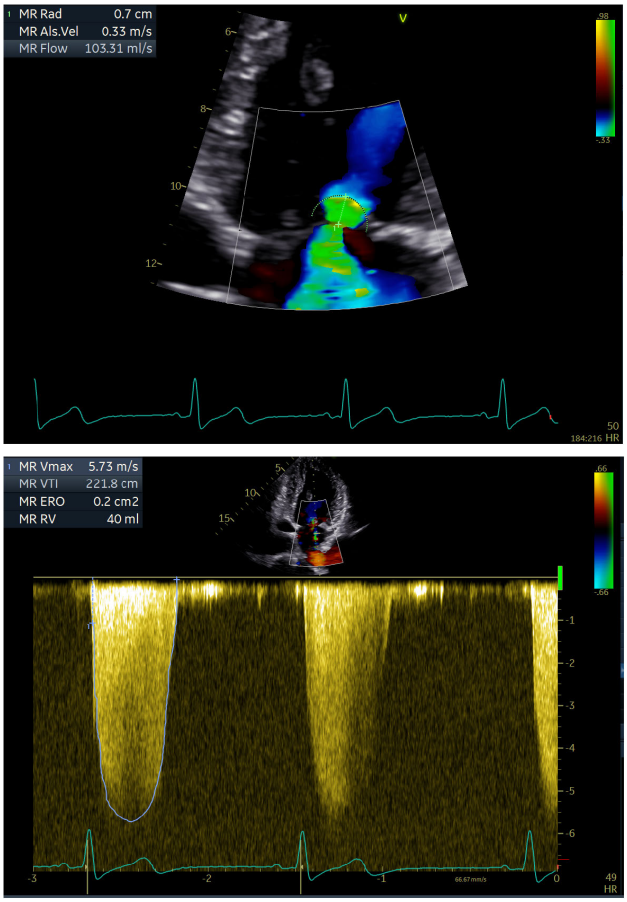

FIGURE 12. 2-D PISA examination results performed by an expert echocardiographer of the same patient shown in Fig. 11. The estimated EROA was 0.2 cm^2 and the estimated RVol was 40 ml. The aliasing velocity used for PISA was 0.33 m/s. The colormap highlights regions with high mean velocity and high variance in green.

can potentially miss the vena contracta. However, because of the principle of conservation of mass, the proposed flow rate estimation method is not sensitive to the imaging depth, provided that it is possible to separate the jet core from the surrounding recruited flow by means of a high-pass filter.

C. AREA ESTIMATION

Of the investigated segmentation strategies, the iterative reconstruction method delivered more consistent and less biased estimates. However, the study pointed out a few limitations that should be discussed. One limitation of the iterative method is that the jet cross section is modelled as an ellipse. This assumption was made to reduce the number of parameters explored by the direct solver and facilitate convergence. However, this assumption may be not applicable in some cases, for example when fused valve cusps generate triangular orifices. In this case the iterative method may provide wrong area estimates or even fail to converge. One solution could be to define the orifice geometry using a linear combination of parametric functions such as B-splines or Bezier curves. On the other hand, the increased number of parameters and their weaker relation with the shape of the final power Doppler image may hinder convergence or increase the chance of meeting local minima. Further work could focus on investigating a new trade-off between generality and robustness, as well as extending the iterative method to cope with bifurcated jets.

Another limitation of the iterative reconstruction method is that it relies on a fast power Doppler simulator that does not take into account the flow characteristics of the jet, but only its spatial extent. The effects of flow recruitment, turbulence and the interaction of the backscattered signal with clutter filtering were not taken into consideration. Analysis of both experimental and clinical data highlighted the importance of suppressing velocity components not associated with the jet core, which can lead to an overestimation of the jet cross-sectional area. These velocity components are most likely associated with flow recruitment or flow picked up by secondary sample volumes in high-PRF acquisitions.

Furthermore, the fast power Doppler simulator is based on the assumptions of long observation windows, which may be weaker in a clinical setting due to movement of the regurgitant jet. Future work could aim at investigating how the flow regime affects the power Doppler depiction of a jet from an orifice of known size, and could be conducted by coupling Computational Fluid Dynamics (CFD) simulations with ultrasound simulations. The study could as well provide the foundation to investigate the optimal clutter filtering strategy and choice of the observation window length.

In silico and phantom results both indicate that the method used for area estimation is critical for the performance of flow rate estimation. Recognising the limitations of the iterative method discussed above, and that there is still potential for improvement in the correspondence between estimated and reference values, the results highlight that segmentation methods based on spatially variant PSF should be preferred to methods based on the assumption of spatially invariant PSF.

D. VELOCITY ESTIMATION

The proposed method uses the mean velocity for the estimation of the instantaneous flow rate. Although the experimental results shown in Fig. 9 and 10 indicate consistent flow rate estimates with reference flow rate measurements, it is not known whether using a mean velocity estimator will perform equally well in patients, due to the possible differences in the flow regimes. Further validation using a CFD model could help investigate the validity of the proposed method in more realistic flow regimes.

It should be noted that the proposed mean velocity estimator is based on the PW Doppler spectrum. The choice of this velocity estimator over a lag-1 autocorrelation estimator was motivated by a number of reasons. First, the autocorrelation estimator can be strongly biased if clutter is not properly filtered, whereas proposed estimator would yield at most a bias equal to half the clutter bandwidth. Second, due to the high bandwidth of the PW Doppler spectra in this application, maximum velocities above twice the Nyquist limit would render velocity estimation impossible. The aliasing properties of the autocorrelation method are therefore not advantageous in this application.

E. CLINICAL FEASIBILITY

The clinical feasibility example shown in Fig. 11 suggests that the proposed method may be used in patients. However, it also revealed challenges related to limited image quality, which may require fine tuning of the processing parameters for every patient to ensure correct tracing of the maximum velocity envelope and tracking of the jet position. Moreover, for this method to be feasible in a clinical routine, the echocardiographer may have to reduce the transmit frequency to prevent aliasing, because of the high velocities associated with the application. The drawback of this measure would be reduced lateral and axial resolution, which already is a limiting factor for the correct estimation of the jet cross-sectional area. Future work could investigate more robust methods to estimate the maximum velocity envelope as well a more robust method to track the displacement of the jet core.

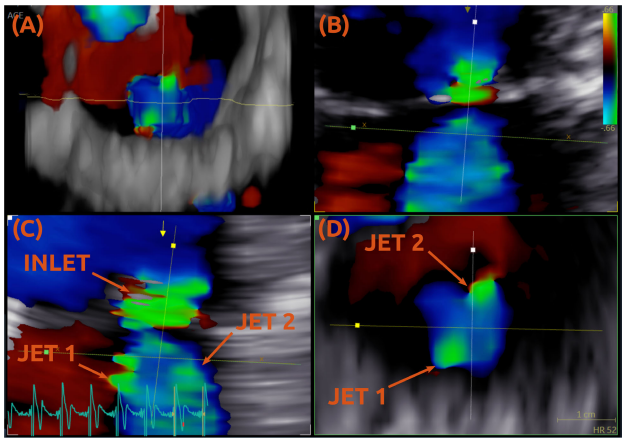

FIGURE 13. **3-D Color Flow image from the same patient shown in Fig. 11 and 12. (A) Cross-sectional view (B) Elevation view (C) Azimuth view (D) Zoomed in cross-sectional view of the jet. The Nyquist velocity was 0.66 m/s. The colormap highlights regions with high mean velocity and high variance in green.**

Comparison with 2-D PISA estimates from the same patient, shown in Fig. 12, showed good Rvol and EROA agreement (48 ml and 0.26 cm^2 compared to 40 ml and 0.2 cm^2 from 2-D PISA). It should be noted that PISA is based on the assumption that blood flows with the maximal velocity in the entire EROA, whereas for the proposed method, the area and mean velocity is estimated in the cross-section of interest and used for flow rate estimation. This means that the proposed method may use different cross-sections for flow rate estimation, but also that the CSA used in the proposed method is not directly related to the EROA derived from PISA. Typically, the former will be larger, depending on the velocity gradients in the cross-section of interest. It should also be noted that PISA measurements are dependent on instantaneous flow rate estimates at selected frames, whereas the proposed framework can account for variations in flow rates and EROA values during the regurgitant phase. For the recording in Fig. 11, the estimated flow rate peaks between 450 ms and 550 ms, when a potential bifurcation is visible in the 3-D color Flow depiction of the jet, shown in Fig. 13. This bifurcation is not detected by the area estimation methods and may thus contribute to a slight overestimation of both regurgitant volume and EROA.

VI. CONCLUSION

In this work we have presented a framework for the estimation of flow rates and flow volumes in aortic and mitral regurgitations. The method combines high frame-rate acquisitions and unfocused beams for the simultaneous estimation of blood velocities and cross-sectional area directly at the jet core. The two estimates are then combined to quantify the instantaneous flow rate. We found that using diverging beams yielded improved estimation accuracy compared with using weakly focused waves, probably because of the more

uniform distribution of the ultrasound energy in the field of view. We also compared two different approaches to segment the jet cross-sectional areas, a thresholding approach and an iterative method. A validation study performed on simulated power Doppler images shows that the iterative method estimates the underlying target size with reduced bias and better consistency compared to a -3 dB threshold ($\beta = 0.97$, $R^2 = 0.91$ and $\beta = 0.8, R^2 = 0.6$, respectively), due to the ability to account for the non uniformity of the PSF. Results are confirmed from recordings of a jet phantom, which show that the iterative method delivers more consistent flow rate estimates compared to a -3 dB threshold ($\beta = 1.2$, $R^2 = 0.88$ and $\beta = 1.16, R^2 = 0.44$, respectively), but also highlight an overestimation bias that should be further investigated. Finally, clinical feasibility was shown in a patient with mitral regurgitation.

REFERENCES

[1] C. M. Otto et al., "2020 ACC/AHA guideline for the management of patients with valvular heart disease: A report of the American College of Cardiology/American Heart Association joint committee on clinical practice guidelines," *J. Amer. College Cardiol.*, vol. 77, no. 4, pp. 25–197, 2021.

[2] H. Baumgartner et al., "2017 ESC/EACTS guidelines for the management of valvular heart disease," *Eur. Heart J.*, vol. 38, no. 36, pp. 2739–2791, 2017.

[3] W. A. Zoghbi et al., "Recommendations for noninvasive evaluation of native valvular regurgitation: A report from the American Society of echocardiography developed in collaboration with the society for cardiovascular magnetic resonance," *J. Amer. Soc. Echocardiography*, vol. 30, no. 4, pp. 303–371, 2017.

[4] P. Lancellotti et al., "Recommendations for the echocardiographic assessment of native valvular regurgitation: An executive summary from the European Association of Cardiovascular imaging," *Eur. Heart J.–Cardiovascular Imag.*, vol. 14, no. 7, pp. 611–644, 2013.

[5] P. Lancellotti et al., "European Association of Echocardiography recommendations for the assessment of valvular regurgitation. Part 2: Mitral and tricuspid regurgitation (native valve disease)," *Eur. J. Echocardiography*, vol. 11, no. 4, pp. 307–332, 2010.

[6] F. Recusani et al., "A new method for quantification of regurgitant flow rate using color Doppler flow imaging of the flow convergence region proximal to a discrete orifice. An in vitro study," *Circulation*, vol. 83, no. 2, pp. 594–604, 1991.

[7] P. M. Vandervoort et al., "Application of color Doppler flow mapping to calculate effective regurgitant orifice area. An in vitro study and initial clinical observations," *Circulation*, vol. 88, no. 3, pp. 1150–1156, 1993.

[8] G. S. Bargiggia et al., "A new method for quantitation of mitral regurgitation based on color flow Doppler imaging of flow convergence proximal to regurgitant orifice," *Circulation*, vol. 84, no. 4, pp. 1481–1489, 1991.

[9] J. M. Rivera, P. M. Vandervoort, D. H. Thoreau, R. A. Levine, A. E. Weyman, and J. D. Thomas, "Quantification of mitral regurgitation with the proximal flow convergence method: A clinical study," *Amer. Heart J.*, vol. 124, no. 5, pp. 1289–1296, Nov. 1992.

[10] J. M. Rivera et al., "Quantification of tricuspid regurgitation by means of the proximal flow convergence method: A clinical study," *Amer. Heart J.*, vol. 127, no. 5, pp. 1354–1362, 1994.

[11] C. M. Tribouilloy, M. Enriquez-Sarano, S. L. Fett, K. R. Bailey, J. B. Seward, and A. J. Tajik, "Application of the proximal flow convergence method to calculate the effective regurgitant orifice area in aortic regurgitation," *J. Amer. College Cardiol.*, vol. 32, no. 4, pp. 1032–1039, Oct. 1998.

[12] W. A. Zoghbi et al., "Recommendations for evaluation of the severity of native valvular regurgitation with two-dimensional and Doppler echocardiography," *J. Amer. Soc. Echocardiography*, vol. 16, no. 7, pp. 777–802, 2003.

[13] P. A. Grayburn, N. J. Weissman, and J. L. Zamorano, "Quantitation of mitral regurgitation," *Circulation*, vol. 126, no. 16, pp. 2005–2017, Oct. 2012.

[14] M. Giesler et al., "Color Doppler echocardiographic determination of mitral regurgitant flow from the proximal velocity profile of the flow convergence region," *Amer. J. Cardiol.*, vol. 71, no. 2, pp. 217–224, 1993.

[15] R. Shandas, M. Gharib, and D. J. Sahn, "Nature of flow acceleration into a finite-sized orifice: Steady and pulsatile flow studies on the flow convergence region using simultaneous ultrasound Doppler flow mapping and laser Doppler velocimetry," *J. Amer. College Cardiol.*, vol. 25, no. 5, pp. 1199–1212, Apr. 1995.

[16] T. Shiota et al., "Effective regurgitant orifice area by the color Doppler flow convergence method for evaluating the severity of chronic aortic regurgitation: An animal study," *Circulation*, vol. 93, no. 3, pp. 594–602, 1996.

[17] M. Enriquez-Sarano, F. A. Miller, S. N. Hayes, K. R. Bailey, A. J. Tajik, and J. B. Seward, "Effective mitral regurgitant orifice area: Clinical use and pitfalls of the proximal isovelocity surface area method," *J. Amer. College Cardiol.*, vol. 25, no. 3, pp. 703–709, Mar. 1995.

[18] T. Buck, B. Plicht, P. Kahlert, I. M. Schenk, P. Hunold, and R. Erbel, "Effect of dynamic flow rate and orifice area on mitral regurgitant stroke volume quantification using the proximal isovelocity surface area method," *J. Amer. College Cardiol.*, vol. 52, no. 9, pp. 767–778, Aug. 2008.

[19] I. A. Simpson, T. Shiota, M. Gharib, and D. J. Sahn, "Current status of flow convergence for clinical applications: Is it a leaning tower of 'PISA?'" *J. Amer. College Cardiol.*, vol. 27, no. 2, pp. 504–509, 1996.

[20] M. Pu, P. M. Vandervoort, N. L. Greenberg, K. A. Powell, B. P. Griffin, and J. D. Thomas, "Impact of wall constraint on velocity distribution in proximal flow convergence zone implications for color Doppler quantification of mitral regurgitation," *J. Amer. College Cardiol.*, vol. 27, no. 3, pp. 706–713, Mar. 1996.

[21] E. G. Cape, J. D. Thomas, A. E. Weyman, A. P. Yoganathan, and R. A. Levine, "Three-dimensional surface geometry correction is required for calculating flow by the proximal isovelocity surface area technique," *J. Amer. Soc. Echocardiography*, vol. 8, no. 5, pp. 585–594, Sep. 1995.

[22] T. Utsunomiya et al., "Doppler color flow 'proximal isovelocity surface area' method for estimating volume flow rate: Effects of orifice shape and machine factors," *J. Amer. College Cardiol.*, vol. 17, no. 5, pp. 1103–1111, 1991.

[23] L. Rodriguez, J. Anconina, F. A. Flachskampf, A. E. Weyman, R. A. Levine, and J. D. Thomas, "Impact of finite orifice size on proximal flow convergence. Implications for Doppler quantification of valvular regurgitation," *Circulat. Res.*, vol. 70, no. 5, pp. 923–930, 1992.

[24] E. G. Cape et al., "Cardiac motion can alter proximal isovelocity surface area calculations of regurgitant flow," *J. Amer. College Cardiol.*, vol. 22, no. 6, pp. 1730–1737, 1993.

[25] J. G. Myers, A. S. Anayiotos, A. M. Elmahdi, G. J. Perry, P. Fan, and N. C. Nanda, "Color Doppler velocity accuracy proximal to regurgitant orifices: Influence of orifice aspect ratio," *Ultrasound Med. Biol.*, vol. 25, no. 5, pp. 771–792, Jun. 1999.

[26] J. Hopmeyer et al., "Estimation of mitral regurgitation with a hemielliptic curve-fitting algorithm: In vitro experiments with native mitral valves," *J. Amer. Soc. Echocardiography*, vol. 11, no. 4, pp. 322–331, 1998.

[27] M. Giesler, G. Grossmann, A. Pfob, D. Bajtay, V. Goller, and V. Hombach, "Color Doppler echocardiography of the flow convergence region in vitro: Effect of the orifice shape on proximal velocity profile," *Zeitschrift fur Kardiologie*, vol. 85, no. 1, pp. 45–52, 1996.

[28] J. Hung, Y. Otsuji, M. D. Handschumacher, E. Schwammenthal, and R. A. Levine, "Mechanism of dynamic regurgitant orifice area variation in functional mitral regurgitation," *J. Amer. College Cardiology*, vol. 33, no. 2, pp. 538–545, Feb. 1999.

[29] E. Schwammenthal, C. Chen, F. Benning, M. Block, G. Breithardt, and R. A. Levine, "Dynamics of mitral regurgitant flow and orifice area. Physiologic application of the proximal flow convergence method: Clinical data and experimental testing," *Circulation*, vol. 90, no. 1, pp. 307–322, 1994.

[30] Y. Topilsky, H. Michelena, V. Bichara, J. Maalouf, D. W. Mahoney, and M. Enriquez-Sarano, "Mitral valve prolapse with mid-late systolic mitral regurgitation," *Circulation*, vol. 125, no. 13, pp. 1643–1651, Apr. 2012.

[31] S. Biner et al., "Reproducibility of proximal isovelocity surface area, vena contracta, and regurgitant jet area for assessment of mitral regurgitation severity," *JACC: Cardiovascular Imag.*, vol. 3, no. 3, pp. 235–243, 2010.

[32] N. Thomas, B. Unsworth, E. A. Ferenczi, J. E. Davies, J. Mayet, and D. P. Francis, "Intraobserver variability in grading severity of repeated identical cases of mitral regurgitation," *Amer. Heart J.*, vol. 156, no. 6, pp. 1089–1094, Dec. 2008.

[33] Y. Matsumura et al., "Geometry of the proximal isovelocity surface area in mitral regurgitation by 3-dimensional color Doppler echocardiography: Difference between functional mitral regurgitation and prolapse regurgitation," *Amer. Heart J.*, vol. 155, no. 2, pp. 231–238, 2008.

[34] Y. Matsumura et al., "Determination of regurgitant orifice area with the use of a new three-dimensional flow convergence geometric assumption in functional mitral regurgitation," *J. Amer. Soc. Echocardiography*, vol. 21, no. 11, pp. 1251–1256, 2008.

[35] C.-H. Yap et al., "Novel method of measuring valvular regurgitation using three-dimensional nonlinear curve fitting of Doppler signals within the flow convergence zone," *IEEE Trans. Ultrason., Ferroelectr., Freq. Control*, vol. 60, no. 7, pp. 1295–1311, Jul. 2013.

[36] E. L. Pierce et al., "Three-dimensional field optimization method: Gold-standard validation of a novel color Doppler method for quantifying mitral regurgitation," *J. Amer. Soc. Echocardiography*, vol. 29, no. 10, pp. 917–925, 2016.

[37] T. C. Tan et al., "Three-dimensional field optimization method: Clinical validation of a novel color Doppler method for quantifying mitral regurgitation," *J. Amer. Soc. Echocardiography*, vol. 29, no. 10, pp. 926–934, 2016.

[38] S. Militaru et al., "Validation of semiautomated quantification of mitral valve regurgitation by three-dimensional color Doppler transesophageal echocardiography," *J. Amer. Soc. Echocardiography*, vol. 33, no. 3, pp. 342–354, 2020.

[39] A. Singh et al., "A novel approach for semiautomated three-dimensional quantification of mitral regurgitant volume reflects a more physiologic approach to mitral regurgitation," *J. Amer. Soc. Echocardiography*, vol. 35, no. 9, pp. 940–946, 2022.

[40] W. R. Brody and J. D. Meindl, "Theoretical analysis of the CW Doppler ultrasonic flowmeter," *IEEE Trans. Biomed. Eng.*, vol. BME-21, no. 3, pp. 183–192, May 1974.

[41] C. F. Hottinger and J. D. Meindl, "Blood flow measurement using the attenuation-compensated volume flowmeter," *Ultrason. Imag.*, vol. 1, no. 1, pp. 1–15, 1979.

[42] B. A. J. Angelsen, "A theoretical study of the scattering of ultrasound from blood," *IEEE Trans. Biomed. Eng.*, vol. BME-27, no. 2, pp. 61–67, Feb. 1980.

[43] T. Buck, R. A. Mucci, J. L. Guerrero, G. Holmvang, M. D. Handschumacher, and R. A. Levine, "The power-velocity integral at the vena contracta," *Circulation*, vol. 102, no. 9, pp. 1053–1061, Aug. 2000.

[44] T. Buck, R. A. Mucci, J. L. Guerrero, G. Holmvang, M. D. Handschumacher, and R. A. Levine, "Flow quantification in valvular heart disease based on the integral of backscattered acoustic power using Doppler ultrasound," *Proc. IEEE*, vol. 88, no. 3, pp. 307–330, Mar. 2000.

[45] T. Buck, B. Plicht, P. Hunold, R. A. Mucci, R. Erbel, and R. A. Levine, "Broad-beam spectral Doppler sonification of the vena contracta using matrix-array technology," *J. Amer. College Cardiol.*, vol. 45, no. 5, pp. 770–779, Mar. 2005.

[46] T. Hergum, T. R. Skaug, K. Matre, and H. Torp, "Quantification of valvular regurgitation area and geometry using HPRF 3-D Doppler," *IEEE Trans. Ultrason., Ferroelectr., Freq. Control*, vol. 56, no. 5, pp. 975–982, May 2009.

[47] T. R. Skaug, T. Hergum, B. H. Amundsen, T. Skjærpe, H. Torp, and B. O. Haugen, "Quantification of mitral regurgitation using high pulse repetition frequency three-dimensional color Doppler," *J. Amer. Soc. Echocardiography*, vol. 23, no. 1, pp. 1–8, Jan. 2010.

[48] T. R. Skaug, B. H. Amundsen, T. Hergum, S. Urheim, H. Torp, and B. O. Haugen, "Quantification of aortic regurgitation using high-pulse repetition frequency three-dimensional colour Doppler," *Eur. Heart J.–Cardiovascular Imag.*, vol. 15, no. 6, pp. 615–622, 2014.

[49] J. Avdal, A. Rodriguez-Molares, E. Andreas Rye Berg, and H. Torp, "Volume flow estimation in valvular jets using 3D high frame rate ultrasound," in *Proc. IEEE Int. Ultrason. Symp. (IUS)*, Oct. 2018, pp. 1–4.

[50] J. C. Lagarias, J. A. Reeds, M. H. Wright, and P. E. Wright, "Convergence properties of the Nelder-Mead simplex method in low dimensions," *SIAM J. Optim.*, vol. 9, no. 1, pp. 112–147, 1998.

[51] J. A. Jensen, "Field: A program for simulating ultrasound systems," *Med. Biol. Eng. Comput.*, vol. 4, no. 1, pp. 351–353, 1996.